

## Fabrication and characterization of thermally drawn fiber capacitors

Guillaume Lestoquoy, Noémie Chocat, Zheng Wang, John D. Joannopoulos, and Yoel Fink

Citation: *Appl. Phys. Lett.* **102**, 152908 (2013); doi: 10.1063/1.4802783

View online: <http://dx.doi.org/10.1063/1.4802783>

View Table of Contents: <http://apl.aip.org/resource/1/APPLAB/v102/i15>

Published by the [American Institute of Physics](#).

---

### Additional information on *Appl. Phys. Lett.*

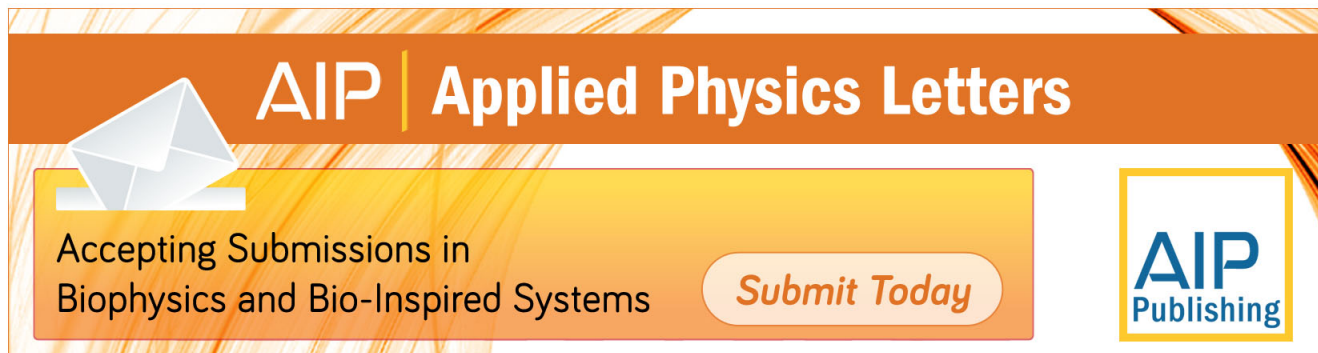
Journal Homepage: <http://apl.aip.org/>

Journal Information: [http://apl.aip.org/about/about\\_the\\_journal](http://apl.aip.org/about/about_the_journal)

Top downloads: [http://apl.aip.org/features/most\\_downloaded](http://apl.aip.org/features/most_downloaded)

Information for Authors: <http://apl.aip.org/authors>

## ADVERTISEMENT



**AIP** | Applied Physics Letters

Accepting Submissions in  
Biophysics and Bio-Inspired Systems

*Submit Today*

**AIP**  
Publishing



## Fabrication and characterization of thermally drawn fiber capacitors

Guillaume Lestoquoy,<sup>1,2,3</sup> Noémie Chocat,<sup>1,2,4,a)</sup> Zheng Wang,<sup>1,2,5,b)</sup>  
John D. Joannopoulos,<sup>1,2,5</sup> and Yoel Fink<sup>1,2,4,c)</sup>

<sup>1</sup>Research Laboratory of Electronics, Massachusetts Institute of Technology, 77 Massachusetts Avenue, Cambridge, Massachusetts 02139, USA

<sup>2</sup>Institute for Soldier Nanotechnologies, Massachusetts Institute of Technology, 77 Massachusetts Avenue, Cambridge, Massachusetts 02139, USA

<sup>3</sup>Department of Electrical Engineering and Computer Science, Massachusetts Institute of Technology, 77 Massachusetts Avenue, Cambridge, Massachusetts 02139, USA

<sup>4</sup>Department of Materials Science and Engineering, Massachusetts Institute of Technology, 77 Massachusetts Avenue, Cambridge, Massachusetts 02139, USA

<sup>5</sup>Department of Physics, Massachusetts Institute of Technology, 77 Massachusetts Avenue, Cambridge, Massachusetts 02139, USA

(Received 3 January 2013; accepted 5 April 2013; published online 19 April 2013)

We report on the fabrication of all-in-fiber capacitors with poly(vinylidene fluoride) (PVDF) as the dielectric material. Electrodes made of conductive polymer are separated by a PVDF thin film within a polycarbonate casing that is thermally drawn into multiple meters of light-weight, readily functional fiber. Capacitive response up to 20 kHz is measured and losses at higher-frequencies are accounted for in a materials-based model. A multilayered architecture in which a folded PVDF film separates interdigitated electrodes over an increased area is fabricated. This structure greatly enhances the capacitance, which scales linearly with the fiber length and is unaffected by fiber dimension fluctuations. © 2013 AIP Publishing LLC [<http://dx.doi.org/10.1063/1.4802783>]

Poly(vinylidene fluoride) (PVDF) is a synthetic polymer used in a wide variety of applications,<sup>1</sup> ranging from ultrasound transducers<sup>2</sup> to lithium ion batteries,<sup>3</sup> thermal sensors,<sup>4</sup> outdoor paints,<sup>5</sup> and western blots.<sup>6</sup> In particular, it is an attractive dielectric material for polymer film capacitors because of its relatively high dielectric constant and strength<sup>7</sup> as well as its potential as matrix for high-permittivity nanocomposite polymers.<sup>8</sup> Such capacitors can achieve high energy densities<sup>9</sup> as well as high strain sensitivity,<sup>10</sup> and the mechanical flexibility of PVDF in these devices presents a great potential for mobile, wearable sensors as well as electrolyte-free energy storage solutions. Yet, although these applications ideally span large areas, the flexibility of PVDF has thus far been exploited in small devices only.<sup>11</sup> The preform-to-fiber thermal-drawing process offers a scalable path to the generation of very large area devices,<sup>12</sup> and recent developments in multi-material fiber fabrication have led to the inclusion of PVDF-based copolymers in piezoelectric fibers for acoustic transduction and optical modulation.<sup>13,14</sup> This opens the way to thermal-drawing of high-permittivity polymer fiber capacitors that are flexible and light-weight. Previous results on polymer fiber capacitors have been reported,<sup>15</sup> but the low permittivity of the polyethylene used limits the capacitance per unit volume of dielectric and the fibers lack a well-integrated metallization scheme. Here, we demonstrate the thermal drawing of a fully functional fiber design containing the dielectric layer as well as both metallic and viscous electrodes. We characterize the

frequency response of the impedance and account for the observed capacitive behavior and its high-frequency limitations in a materials-based model. A multilayered design comprising a wider, folded PVDF film is then demonstrated and is shown to greatly enhance the capacitance, which scales linearly with the fiber length and is unaffected by possible dimension fluctuations during the draw process.

The simplest capacitor architecture involves two planar parallel electrodes separated by an insulating material. In that case, the capacitance is given by

$$C = \frac{\epsilon_d A}{t}, \quad (1)$$

where  $\epsilon_d$  is the absolute permittivity of the dielectric layer and  $t$  its thickness, while  $A$  is the area over which the electrodes are facing. Large capacitance is, therefore, obtained by placing a thin film of high-permittivity material between conductive domains over a wide surface. The thermal-draw process, in which a macroscopic preform can yield kilometers of axially invariant fiber, is well suited to achieve such large areas. Remarkably, the process leaves the cross-sectional aspect-ratio of all the fiber features unchanged. We, therefore, see from Eq. (1) that for a given length of fiber containing such a flat capacitor structure, the ratio  $A/t$  should not depend on the fiber's final dimensions. The capacitance per unit length is thus entirely set by the chosen dielectric film thickness and width in the preform, allowing the capacitance per unit volume—or per unit weight—of the fiber to be greatly increased as it is drawn thinner.

Thanks to its high permittivity as a polymer—around  $10 \epsilon_0$  at room temperature and 1 kHz (Ref. 16)—PVDF is a good candidate to achieve high capacitance. However, the choice of PVDF as dielectric material is a challenging one.

<sup>a)</sup>Present address: Thin Film Department, Saint-Gobain Recherche, 39 quai Lucien Lefranc, 93303 Aubervilliers, France.

<sup>b)</sup>Present address: Department of Electrical and Computer Engineering, University of Texas at Austin, Austin, Texas 78712, USA.

<sup>c)</sup>Electronic mail: yoel@mit.edu

Indeed, while most polymers routinely used in fiber drawing have high glass-transition temperature and a viscosity that continuously decreases with increased temperature,<sup>12</sup> PVDF, a semi-crystalline polymer, melts at a temperature between 158 °C and 197 °C.<sup>17</sup> Such a material is traditionally challenging to draw as a thin layer within a fiber, since large-aspect-ratio, low-viscosity elements are subject to capillary instabilities due to surface tension and can ultimately break-up into smaller elements.<sup>18</sup> Drawing of a thin layer of PVDF thus necessitates its confinement within boundaries that remain viscous enough during the draw process. In a capacitor, these boundaries are the electrodes, which must, therefore, be both viscous and conductive. Commonly employed crystalline metals are thus unsuitable, and we instead use a composite polymer loaded with carbon particles, Conductive Polyethylene (CPE). Its viscosity enables the drawing of large aspect ratio electrodes that can confine the liquefied PVDF.<sup>13</sup> Figs. 1(a)–1(d) depict the process of fabrication of a flat capacitor fiber by scaling down of a macroscopic preform using thermal drawing. Initially, a 5 mm-thick bar of polycarbonate (McMaster) is milled to the proper shape and a strip of Bi<sub>58</sub>Sn<sub>42</sub> (eutectic alloy, Indium Corporation) is inserted in it. A 400 μm-thick CPE sheet (Measurement Specialties) is then wrapped around the rounded edge of the bar and the whole operation is repeated a second time. These two identically prepared elements are then stacked around a 300 μm thick PVDF layer (AJEDIUM Film Group, Solef 10.0) and the structure is consolidated under vacuum at ~185 °C. The obtained preform (38 mm wide, 11 mm thick, and 200 mm long) is then thermally drawn at ~230 °C into tens of meters of flexible fiber. The optical micrograph in

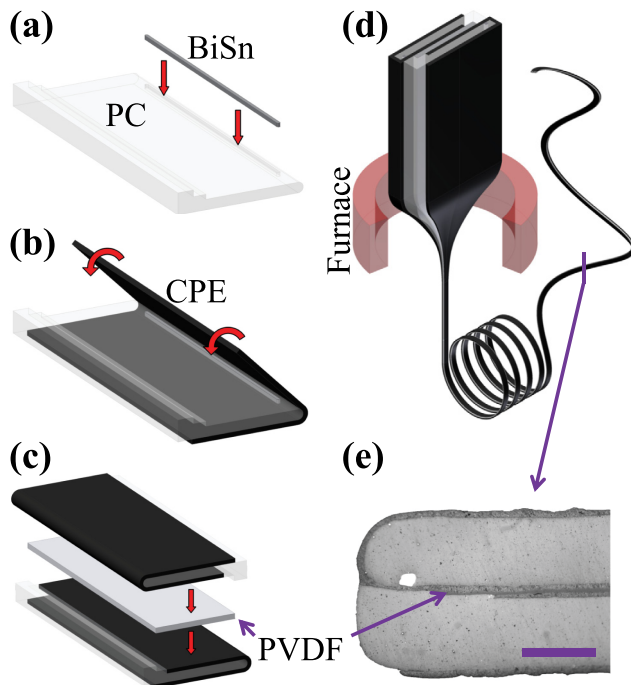


FIG. 1. Fiber fabrication. (a)–(d) Fabrication process flow. (e) Optical micrograph of the fiber cross-section: The central PVDF layer is flanked by two layers of CPE (dark gray), wrapped around the surrounding PC (light gray) bars to cover the fiber sides (top and bottom). The Bi<sub>58</sub>Sn<sub>42</sub> wire is shown in white. Scale bar in (e) is 200 μm.

Fig. 1(e) depicts the key elements of the fiber cross section: the flat central capacitor structure, the wrapped CPE layers allowing easy electrical connection from the outside and the integrated metallic bus, added to ensure good electrical conduction along potentially extended fiber lengths. Indeed, the conductivity of CPE (1–10 S m<sup>-1</sup>),<sup>14</sup> while well-suited for conduction within the millimetric fiber cross-section, is not sufficient to ensure a uniform electric potential along meters of fiber.<sup>19</sup> While this effect can be exploited in some cases,<sup>19,20</sup> here it would preclude long fibers from behaving as capacitors (see supplementary Fig. 1).<sup>27</sup>

The fiber capacitive behavior can be demonstrated from the variations of the fiber complex impedance  $Z$  with  $f$ , the ac frequency of the applied voltage. Using a Hioki 3532-50 LCR HiTester impedance analyzer directly connected to the fiber sides, we record these variations over the [42 Hz; 5 MHz] range. Fig. 2(a) depicts both the measured modulus  $|Z|$  and phase  $\varphi$  of  $Z$  as  $f$  varies. For an ideal capacitor,  $|Z|$  would be inversely proportional to  $f$ , and  $\varphi$ , the phase shift between voltage and current, equal to  $-90^\circ$  at all frequencies. In practice, however, capacitors depart from this ideal behavior

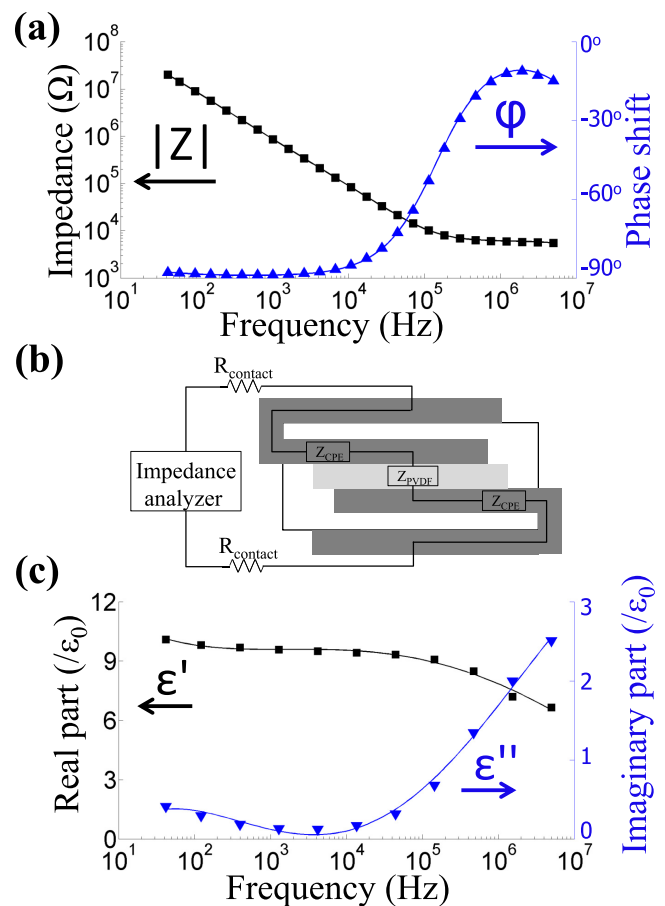


FIG. 2. Fiber frequency response and materials-based model. (a) Frequency response of the impedance of a 2.4 cm flat capacitor fiber sample. Black squares represent the measured complex impedance modulus (left axis) and blue triangles its phase (right axis). Black and blue lines are resp. the modeled behavior of  $|Z|$  and  $\varphi$  using the model shown in (b) and the polynomial functions obtained from (c). (b) Schematic model of a fiber connected to an impedance analyzer. (c) Frequency dependence of  $\epsilon_{pvdf}$  of a 300 μm-thick film before thermal draw. Black squares represent the measured real part (left axis) and blue triangles the measured imaginary part (right axis). Solid black and blue lines are 4th order polynomial approximations of these data.

because of their internal series resistance, which prevents  $|Z|$  from dropping indefinitely with  $f$  and reduces  $\varphi$ , and because of current leakage through the dielectric material, which also impacts  $\varphi$ . The quality of the capacitor can be estimated by the dissipation factor DF, defined as<sup>21</sup>

$$DF = \tan(\varphi + 90^\circ). \quad (2)$$

We see in Fig. 2(a) that DF reaches 10% (for  $\varphi = 84^\circ$ ) at 20 kHz and 50% (for  $\varphi = 63^\circ$ ) around 100 kHz, beyond which  $|Z|$  plateaus and  $\varphi$  drops significantly, setting the upper limit on the frequency of operation of the fiber as a capacitor.

In order to properly identify the origin of these limitations of the capacitor performances, we construct a model for  $Z$  that takes the different materials' behaviors into account. Thanks to the conductive  $\text{Bi}_{58}\text{Sn}_{42}$  elements, the fiber behaves like a simple series circuit as depicted schematically in Fig. 2(b), in which  $Z$  is modeled as the sum of the impedances of the different parts of the system:  $Z_{CPE}$  for the polymer electrodes,  $Z_{PVDF}$  for the PVDF film, and a purely resistive term  $R_{contact}$  to take into account losses at the connection with the setup. It has been reported that because of its composite nature, the resistivity of CPE is stable at low frequency but decreases above a critical frequency  $f_0$ , whose value highly depends on the polymer treatment.<sup>22</sup> We take this into account by modeling the  $Z_{CPE}(f)$  in the following way:

$$Z_{CPE}(f) = \frac{R_{CPE}}{1 + j\frac{f}{f_0}}, \quad (3)$$

where  $R_{CPE}$  is the low frequency resistance of the electrode. We have repeatedly witnessed this effect in fibers containing CPE and, because the thermal-drawing process itself can greatly impact the value of  $f_0$ , we take it as a parameter in this model. The impedance of the PVDF layer is calculated using Eq. (1)

$$Z_{PVDF}(f) = \frac{1}{j\frac{A\varepsilon_{pvdf}}{t}2\pi f}, \quad (4)$$

where  $A$ ,  $t$ , and  $\varepsilon_{pvdf}$  are, respectively, the surface area, thickness, and dielectric permittivity of the PVDF film inside the fiber. The overall impedance of the system is obtained by summing its constituent parts

$$Z(f) = 2R_{contact} + 2Z_{CPE}(f) + Z_{PVDF}(f). \quad (5)$$

As seen in Eq. (4),  $\varepsilon_{pvdf}$  is central in setting the capacitance of the fiber device and its variations with the frequency  $f$  are expected to impact the fiber response. We measure these variations by gold-coating both sides of a  $1 \text{ cm}^2$  portion of a  $300 \mu\text{m}$ -thick film of PVDF such as the one placed in the preform, and using the same impedance analyzer as previously. From the measured data and Eq. (4), we retrieve the variations of  $\varepsilon_{pvdf}$  with  $f$  and show the obtained results in Fig. 2(c) for  $\varepsilon'$  and  $\varepsilon''$ , respectively, the real and imaginary parts of  $\varepsilon_{pvdf}$ , which are consistent with similar reported measurements.<sup>16</sup> Using MATLAB, the discrete data points obtained are modeled by two fourth-order polynomial functions, shown in

solid lines on this same plot. Although these functions capture accurately the variations of  $\varepsilon'$  and  $\varepsilon''$  over the range of frequencies of interest for the PVDF film used in the preform, the drawing process is likely to alter  $\varepsilon_{pvdf}$  as PVDF melts and recrystallizes.<sup>16</sup> In our model, we include this effect by keeping  $\varepsilon'$  (1 kHz) and  $\varepsilon''$  (1 kHz) as parameters, and variations of  $\varepsilon_{pvdf}$  with  $f$  are assumed to follow the polynomial functions obtained earlier, but scaled proportionally to the change of PVDF permittivity at 1 kHz from the preform to the fiber. The result of fitting (5) to the measured impedance of the fiber sample is displayed in Fig. 2(a). The quality of the fit is excellent for [ $R_{contact} = 2.8 \text{ k}\Omega$ ,  $R_{CPE} = 3.0 \text{ k}\Omega$ ,  $f_0 = 10.5 \text{ MHz}$ ,  $\varepsilon'$  (1 kHz) =  $12.7\varepsilon_0$ , and  $\varepsilon''$  (1 kHz) =  $0.14\varepsilon_0$ ], a set of values consistent with previously reported results,<sup>14</sup> which indicates a slight increase of the permittivity of PVDF induced by the draw process itself. This model shows that the plateau in  $|Z|$  at high frequencies can be lowered by arranging the geometry of the fiber in order to reduce  $R_{CPE}$ , so that the ultimate limitation in this fiber is the increased dielectric loss  $\varepsilon''$  in PVDF above 100 kHz.

To increase the fiber capacitance, the dielectric constant of the dielectric layer could be modified. Indeed, nanocomposite materials using PVDF or its co- or ter-polymers as matrix, filled with various ceramic, metallic, or organic particles are the center of an active area of research,<sup>8</sup> and dielectric constants in the hundreds have already been achieved.<sup>23–25</sup> However, the fillers in such composites do not only impact the permittivity but also the dielectric strength and, importantly, the mechanical properties of the polymer. Identifying nanocomposite polymers with high permittivity and dielectric strength that remain compatible with the thermal-drawing process calls for a wide-scale study that is beyond the scope of this paper. Nonetheless, other strategies can be developed to enhance the fiber capacitance without replacing the dielectric material. A thinner layer of PVDF can be used, although its low viscosity during the draw makes thinning it down below a few microns challenging. A more efficient strategy consists in increasing the electrodes' surface area per unit length of fiber, by expanding the fraction of fiber volume taken by the capacitive structure. In Fig. 3, we show an evolved fiber design, in which the internal architecture of the fiber is made of interdigitated CPE electrodes, separated by a folded PVDF film. This structure is inspired from multilayered ceramic capacitors,<sup>26</sup> as it yields large effective electrode area per unit volume and can easily be reproduced with polymer films. As shown in Fig. 3(a), the fabrication process differs from the one shown in Fig. 1 only in the fact that a multilayered structure is now placed between the prepared PC bars instead of a single layer of PVDF. The rest of the fiber fabrication process is identical, and a typical cross-section of the obtained fiber is shown in Fig. 3(b) for a structure where the PVDF layer is folded 6 times. Fig. 3(c) shows the tip of the CPE "fingers" and demonstrates that PVDF maintains its structural integrity during the draw. With this approach, fiber capacitors with much greater internal surface area of electrode can be produced, and the active volume inside the fiber is increased as well. To demonstrate the efficiency of this strategy in enhancing the fiber capacitance, three preforms with different architectures were fabricated

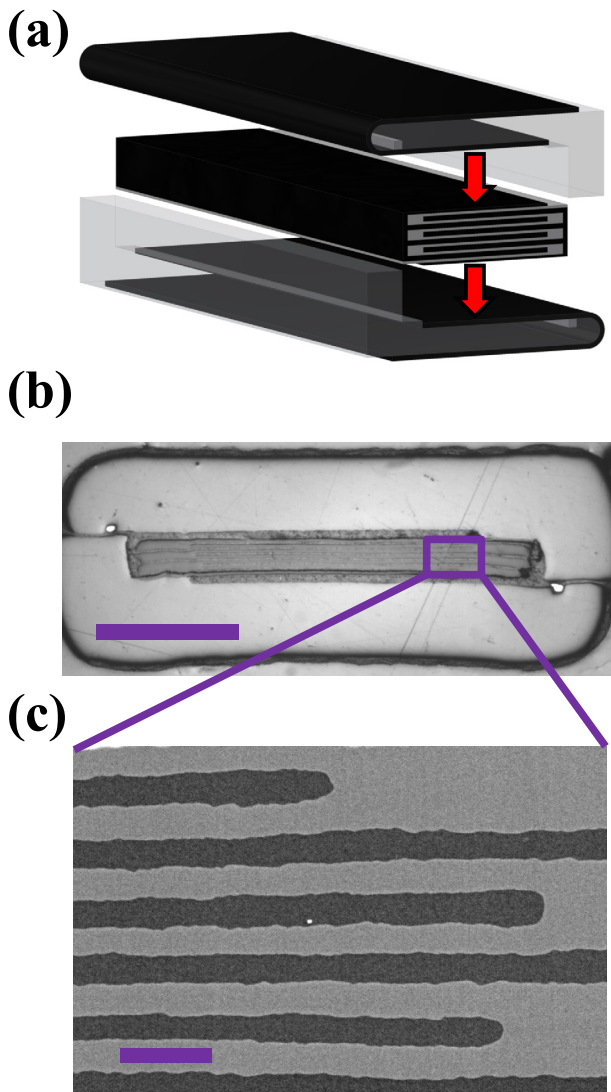


FIG. 3. Large-active-area fiber design. (a) A multilayered structure of interdigitated CPE layers separated by a PVDF thin-film replaces the single layer of PVDF of Fig. 1(c) in the fabrication process, otherwise unchanged. (b) Optical micrograph of a fiber cross-sectional structure containing a 6-fold PVDF structure as depicted in (a). (c) SEM micrograph of the layered structure: The CPE “fingers” (dark gray) are separated by the folded PVDF layer (light gray). Scale bars are  $300\ \mu\text{m}$  in (b) and  $20\ \mu\text{m}$  in (c).

and drawn into fibers. The first contained a single  $300\ \mu\text{m}$ -thick PVDF film as depicted in Fig. 1, with CPE electrodes facing over 18 mm in the preform cross-section. The second one had a twice-folded  $225\ \mu\text{m}$ -thick PVDF film, separating a width of 60 mm of CPE electrodes. The last was the one depicted in Fig. 3, with a six-times-folded  $300\ \mu\text{m}$ -thick PVDF film, spanning 126 mm in electrode width. Using Eq. (1) and the in-fiber PVDF dielectric constant of  $12.7\ \epsilon_0$  obtained from the previous model at 1 kHz yields expected capacitance per unit length values of, respectively,  $6.7\ \text{nF m}^{-1}$ ,  $30\ \text{nF m}^{-1}$ , and  $47\ \text{nF m}^{-1}$  for these three fibers. In Fig. 4, we display the measured capacitance of fiber samples as a function of their length for these three architectures. The values obtained from the linear fit to the data points are, respectively,  $6\ \text{nF m}^{-1}$ ,  $32\ \text{nF m}^{-1}$ , and  $49\ \text{nF m}^{-1}$ , in excellent agreement with the predictions, which indicates limited variations in the way PVDF crystallizes at the end of the drawing process from one fiber to the next and a maintained

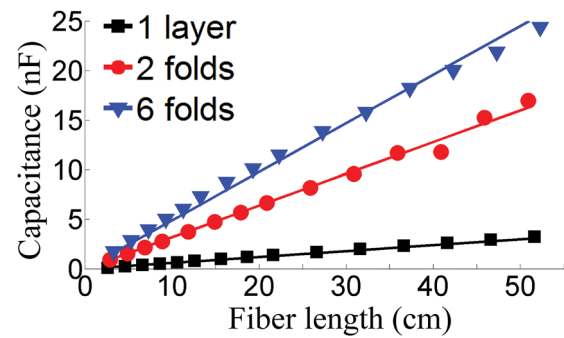


FIG. 4. Measured capacitance of fiber samples as a function of the fiber length for 3 different designs: single-layer (black squares), twice-folded (red circles) and six-times-folded (blue triangles) PVDF thin-film. The straight lines are linear fits to the data, with slopes of  $6\ \text{nF m}^{-1}$ ,  $32\ \text{nF m}^{-1}$ , and  $49\ \text{nF m}^{-1}$ , respectively.

aspect ratio of the drawn PVDF film from preform to fiber. Indeed, for each fiber, the tested samples had variable cross-sectional dimensions, and these measurements validate the independence of the linear capacitance on these fluctuations. The result on Fig. 4 demonstrates the validity of the multilayered approach in enhancing the fiber capacitance, as this method can be scaled so as to increase even more the active volume within the fiber.

In summary, we have demonstrated an all-in-fiber capacitor using PVDF as dielectric material. The low-loss capacitive behavior up to 20 kHz of the device is established and the high-frequency behavior is accounted for by the materials' properties. Using CPE, a viscous conductive material for the electrodes, multilayered structures comprised high aspect ratio films are drawn and it yields high capacitance that scales linearly with the fiber length.

This work was supported in part by the Materials Research Science and Engineering Program of the U.S. National Science Foundation under Award No. DMR-0819762 and also in part by the U.S. Army Research Office through the Institute for Soldier Nanotechnologies under Contract No. W911NF-07-D-0004.

- <sup>1</sup>S. B. Lang and S. Muensit, *Appl. Phys. A* **85**, 125 (2006).
- <sup>2</sup>Q. Chen and P. Payne, *Meas. Sci. Technol.* **6**, 249 (1995).
- <sup>3</sup>J. Y. Song, Y. Y. Wang, and C. C. Wan, *J. Power Sources* **77**, 183 (1999).
- <sup>4</sup>N. Fujitsuka, J. Sakata, Y. Miyachi, K. Mizuno, K. Ohtsuka, Y. Taga, and O. Tabata, *Sens. Actuators, A* **66**, 237 (1998).
- <sup>5</sup>J. Faucheu, K. Wood, L. Sung, and J. Martin, *JCT Res.* **3**, 29 (2006).
- <sup>6</sup>P. Matsudaira, *J. Biol. Chem.* **262**, 10035 (1987).
- <sup>7</sup>T. R. Jow and P. J. Cygan, *J. Appl. Phys.* **73**, 5147 (1993).
- <sup>8</sup>P. Barber, S. Balasubramanian, Y. Anguchamy, S. Gong, A. Wibowo, H. Gao, H. J. Ploehn, and H.-C. Zur Loye, *Materials* **2**, 1697 (2009).
- <sup>9</sup>B. Chu, X. Zhou, K. Ren, B. Neese, M. Lin, Q. Wang, F. Bauer, and Q. M. Zhang, *Science* **313**, 334 (2006).
- <sup>10</sup>K. I. Arshak, D. McDonagh, and M. A. Durcan, *Sens. Actuators* **79**, 102 (2000).
- <sup>11</sup>K. Arshak, D. Morris, A. Arshak, O. Korostynska, and K. Kaneswaran, in *29th International Spring Seminar on Electronics Technology, St. Marienthal, Germany, 10–14 May 2006* (IEEE Conference Publications, 2006), pp. 334–339.
- <sup>12</sup>A. Abouraddy, M. Bayindir, G. Benoit, S. Hart, K. Kuriki, N. Orf, O. Shapira, F. Sorin, B. Temelkuran, and Y. Fink, *Nature Mater.* **6**, 336 (2007).
- <sup>13</sup>S. Egusa, Z. Wang, N. Chocat, Z. M. Ruff, A. M. Stolyarov, D. Shemuly, F. Sorin, P. T. Rakich, J. D. Joannopoulos, and Y. Fink, *Nature Mater.* **9**, 643 (2010).
- <sup>14</sup>N. Chocat, G. Lestoquoy, Z. Wang, D. M. Rodgers, J. D. Joannopoulos, and Y. Fink, *Adv. Mater.* **24**, 5327 (2012).

- <sup>15</sup>J. F. Gu, S. Gorgutsa, and M. Skorobogatiy, *Appl. Phys. Lett.* **97**, 133305 (2010); *Smart Mater. Struct.* **19**, 115006 (2010).
- <sup>16</sup>R. Gregorio and E. Ueno, *J. Mater. Sci.* **34**, 4489 (1999).
- <sup>17</sup>*Modern Fluoropolymers*, edited by D. A. Seiler and J. Scheirs (Wiley, New York, 1997), pp. 487–506.
- <sup>18</sup>D. S. Deng, N. D. Orf, A. F. Abouraddy, A. M. Stolyarov, J. D. Joannopoulos, H. A. Stone, and Y. Fink, *Nano Lett.* **8**, 4265 (2008).
- <sup>19</sup>F. Sorin, G. Lestoquoy, S. Danto, J. D. Joannopoulos, and Y. Fink, *Opt. Express* **18**, 24264 (2010).
- <sup>20</sup>A. M. Stolyarov, L. Wei, F. Sorin, G. Lestoquoy, J. D. Joannopoulos, and Y. Fink, *Appl. Phys. Lett.* **101**, 011108 (2012).
- <sup>21</sup>R. Kotz and M. Carlen, *Electrochim. Acta* **45**, 2483 (2000).
- <sup>22</sup>*Carbon Black–Polymer Composites: The Physics of Electrically Conducting Composites*, edited by H. Kawamoto and E. K. Sichel (Marcel Dekker, New York, 1982), pp. 135–162.
- <sup>23</sup>Z.-M. Dang, Y.-H. Lin, and C.-W. Nan, *Adv. Mater.* **15**, 1625 (2003).
- <sup>24</sup>M. Arbatti, X. Shan, and Z.-Y. Cheng, *Adv. Mater.* **19**, 1369 (2007).
- <sup>25</sup>Q. Zhang, H. Li, M. Poh, F. Xia, Z. Cheng, H. Xu, and C. Huang, *Nature* **419**, 284 (2002).
- <sup>26</sup>H. Kishi, Y. Mizuno, and H. Chazono, *Jpn. J. Appl. Phys., Part 1* **42**, 1 (2003).
- <sup>27</sup>See supplementary material at <http://dx.doi.org/10.1063/1.4802783> for evidence of the need for metallic current buses along the fiber length and for details on the behavior of longer fiber samples with frequency.